Published in final edited form as:
Glia. 2013 June ; 61(6): 855–868. doi:10.1002/glia.22479.

NADPH oxidase and aging drive microglial activation, oxidative stress and dopaminergic neurodegeneration following systemic LPS administration

Liya Qin[1], **Yuxin Liu**[4], **Jau-Shyong Hong**[5], and **Fulton T. Crews**[1,2,3,*]

[1]Bowles Center for Alcohol Studies, University of North Carolina School of Medicine, CB#7178, Chapel Hill, NC 27599-7178

[2]Department of Psychiatry, University of North Carolina School of Medicine, CB#7178, Chapel Hill, NC 27599-7178

[3]Department of Pharmacology, University of North Carolina School of Medicine, CB#7178, Chapel Hill, NC 27599-7178

[4]Laboratory of Cell Pharmacology, School of Pharmaceutical Sciences, Hebei University, PR China

[5]Neuropharmacology Section, NIEHS, RTP, NC 27709

Abstract

Parkinson's disease is characterized by a progressive degeneration of substantia nigra (SN) dopaminergic neurons with age. We previously found that a single systemic lipopolysaccharide (LPS, 5 mg/kg, i.p.) injection caused a slow progressive loss of tyrosine hydroxylase immunoreactive (TH+IR) neurons in SN associated with increasing motor dysfunction. In this study, we investigated the role of NADPH oxidase (NOX) in inflammation-mediated SN neurotoxicity. A comparison of control ($NOX2^{+/+}$) mice with NOX subunit $gp91^{phox}$-deficient ($NOX2^{-/-}$) mice 10 months after LPS administration (5 mg/kg, i.p.) resulted in a 39% ($p<0.01$) loss of TH+IR neurons in $NOX2^{+/+}$ mice, whereas, $NOX2^{-/-}$ mice did not show a significant decrease. Microglia (Iba1+IR) showed morphological activation in $NOX2^{+/+}$ mice, but not in $NOX2^{-/-}$ mice at 1 hour. Treatment of $NOX2^{+/+}$ mice with LPS resulted in a 12 fold increase in NOX2 mRNA in midbrain and 5.5–6.5 fold increases in NOX2 protein (+IR) in SN compared to the saline controls. Brain reactive oxygen species (ROS), determined by hydroethidine histochemistry, was increased by LPS in SN between 1 hour and 20 months. Diphenyliodonium (DPI), a NOX inhibitor, blocked LPS-induced activation of microglia and production of ROS, TNFα, IL-1β, and MCP-1. Although LPS increased microglial activation and ROS at all ages studied, saline control $NOX2^{+/+}$ mice showed age-related increases in microglial activation, NOX and ROS levels at 12 and 22 months of age. Together, these results suggest that NOX contributes to persistent microglial activation, ROS production and dopaminergic neurodegeneration that persist and continue to increase with age.

Keywords

neuroimmune; senescence; Parkinson's disease; substantia nigra; endotoxin

*Corresponding Author: Fulton T. Crews, Director, Bowles Center for Alcohol Studies, The University of North Carolina at Chapel Hill, 1021 Thurston Bowles Building, CB 7178, Chapel Hill, NC 27599-7178, Phone: 919-966-5678, Fax: 919-966-5679, ftcrews@med.unc.edu, http://www.med.unc.edu/alcohol/.

INTRODUCTION

Parkinson's disease (PD) is a neurodegenerative movement disorder common in the elderly with most cases occurring after the age of 50. The loss of movement in PD is associated with a progressive loss of dopaminergic neurons in the substantia nigra (SN). Increasing evidence has demonstrated that neuroinflammation is a prominent contributor to the pathogenesis of progressive PD (Block and Hong 2007; Hirsch and Hunot 2009; McGeer et al. 2001; Qian et al. 2010). Previously, we reported that a single systemic injection of LPS produced a persistent neuroimmune response that over months resulted in a loss of SN neurons (Qin et al. 2007) and that LPS induced progressive SN neurodegeneration was associated with motor function deficits reversible with L-DOPA (Liu et al. 2008; Qin et al. 2007). Our findings suggest that initial microglial activation amplifies glial neuroimmune responses resulting in persistent increases in innate immune gene expression, e.g. proinflammatory cytokines, oxidases and proteases (Qin et al. 2008; Qin et al. 2007). In this report we test the hypothesis that NADPH oxidase (NOX), specifically (NOX2), contributes to persistent microglial activation, reactive oxygen species (ROS) formation and SN neurodegeneration.

NADPH oxidase (NOX) is a series of enzymes that are involved in producing ROS. The most studied NOX enzyme, NOX2, also known as $gp91^{phox}$, and phagocyte oxidase (PHOX) is highly expressed in innate immune cells including microglia. Innate immune gene induction in brain involves positive loops of proinflammatory gene induction that converge upon the transcription factor NF-κB. NF-κB transcription is activated by kinases as well as ROS (Crews et al. 2011). ROS has long been recognized as a contributor to chronic progression of neurodegenerative diseases (Dauer and Przedborski 2003; Glass et al. 2010). Chronic neurodegenerative diseases, including Parkinsonism, occur primarily in the elderly suggesting age and/or time contribute to disease progression. Studies in mixed neuronal-glial cultures have found that NOX2 contributes to ROS formation, microglial activation and dopamine (DA) neuron degeneration (Gao et al. 2003; Qin et al. 2004). However, how NOX2 contributes to degeneration in vivo is poorly understood. To better understand the interaction of microglial activation, NOX and neurodegeneration, we investigated mice at various times during increasing age following lipopolysaccharide (LPS) induced neuroimmune activation of microglia and NOX2 induction. We report here that NOX2 contributes to the initiation and persistence of microglial activation and ROS formation for months that contributes to SN neurodegeneration. Increasing age is further found to increase microglial activation morphology, NOX2 expression and ROS formation. The combination of persistent LPS neuroimmune activation and increasing age amplifies ROS accelerating age related neurodegeneration. These studies suggest that NOX2 makes an important contribution of persistent microglial activation, ROS production and SN neurodegeneration.

MATERIALS AND METHODS

Animals

Eight-week-old male (25–30 g) and female (25–30 g) B6.129S6-*Cybb*^{tm1Din} ($NOX2^{-/-}$) and C57BL/6J 000664 ($NOX2^{+/+}$) mice were purchased from Jackson Laboratories (Bar Harbor, ME). B6.129S6-*Cybb*^{tm1Din} $NOX2^{-/-}$ mice lack a functional gp91 protein, an X chromosome gene that contains the catalytic subunit of the NOX complex. The $NOX2^{-/-}$ mutation is maintained in the C57BL/6J background; therefore, C57BL/6J ($NOX2^{+/+}$) mice were used as control animals. Breeding of the mice was performed to achieve eight-week-old animals. Male mice were randomly assigned to different groups and treated according to each group protocol. All protocols in this study were approved by the Institutional Animal

Care and Use Committee and were in accordance with the National Institute of Health regulations for the care and use of animals in research.

Reagents

Lipopolysaccharide (LPS, strain O111:B4) was purchased from Calbiochem (San Diego, CA). Hydroethidine was from Invitrogen Molecular Probes (Eugene, OR). TNFα, IL-1β and MCP-1 ELISA kits were purchased from R & D Systems Inc. (Minneapolis, MN). All other reagents came from Sigma Chemical Co. (St. Louis, MO). Antibodies used in this study are shown in Table 1.

Animal treatment

Male C57BL/6J ($NOX2^{+/+}$) and Cybb ($NOX2^{-/-}$) mice were intraperitoneally injected with a single dose of LPS (5 mg/kg) or vehicle (0.9% saline). The dosage of LPS used (5 mg/kg, i.p.) was based on our previous study of endotoxic shock and the loss of dopaminergic neurons (Li et al. 2005). Mice were sacrificed at the time points indicated and brains were used for mRNA, protein, and morphological analyses. For NOX inhibitor studies, male C57BL/6 mice were treated with LPS (5 mg/kg, i.p.) or saline. Diphenyleneiodonium (DPI, 3 mg/kg) was injected intraperitoneally on two consecutive days 2 months after LPS treatment. Mice were sacrificed 3 hr after the last dose of DPI. Brains were used for protein and morphological study. Procedures using laboratory animals were in accordance with the National Institutes of Health guidelines for the use of live animals and approved by IUCAC boards.

Analysis of neurotoxicity

The loss of dopaminergic neurons was assessed by counting the number of TH +immunoreactive (TH+IR) neurons in the substantia nigra pars compacta (SNpc) region by 2 individuals who were blind to the treatment using the CAST stereological system. The boundary between the SNpc and the adjacent ventral tagmental area was defined using (Paxinos and Franklin 2004). To ensure the accuracy of the count, a normal distribution (rostral to caudal) of SNpc TH+IR neurons was first established in the control mice (Zhang et al. 2004). In brief, we determined the number of SNpc TH+IR neurons for each of the 24 consecutive coronal sections that encompass the entire SN. Counts from 4 animals for each sham-control group of $NOX2^{+/+}$ and $NOX2^{-/-}$ mice were averaged to create a normal distribution curve. No significant differences were observed in the distribution patterns for SNpc TH+IR neurons between $NOX2^{+/+}$ and $NOX2^{-/-}$ mice. A change in SN size could lead to an underestimation of cell death, although our studies did not detect a global loss of SN size. To count the number of SNpc TH+IR neurons in the saline and LPS-injected mice, we used the first (rostral) and every forth section of the 24 sections of each brain (i.e., 8 sections/brain) for the counting. The distribution of the SNpc TH+IR neurons in each set of brain sections was compared with that of its respective sham-control to correct for potential "frame-shifting" errors resulting from brain slicing and assignment of the first of the 24 sections. A mean value for the number of SNpc TH+IR neurons was then deduced by averaging the counts of the 8 sections for each animal; the results were expressed as the average number of SNpc TH+IR neurons per section as described previously (Zhang et al. 2004)

Microscopic quantification

Two quantification methods were used to measure levels of immunostaining and fluorescent staining. 1. Intensity of NOX2 immunoreactivity and ethidium fluorescence was measured by BioQuant image analysis software (Nashville, TN). Images were captured on an Olympus BX51 microscope and Sony DCX-390 video camera at 40X. Light levels were

normalized to preset levels and the microscope, camera, and software were background corrected to ensure reliability of image acquisition (Crews et al. 2004). Eight random images from each brain section were captured within the substantia nigra (SN), the intensity of immunostaining and fluorescence was measured in pixels within this area and expressed as pixels/mm^2. Subsequently, the average of the eight measurements was used to represent the intensity of immunoreactivity or fluorescence of each section. Six sections were measured per animal. When measuring the intensity of NOX2+IR and ethidium fluorescence in the cells, we eliminated the background by adjusting threshold to avoid background staining. 2. Number of TH+IR and Iba1+IR cells was counted using a modified stereological technique in the substantia nigra pars compacta (SNpc) of immunostained brain sections using the CAST stereological system (Chen et al. 1998; McClain et al. 2011; Qin and Crews 2012a). For confocal microscopy, triple labeled sections were digitally photographed with Leica SP2-AOBS confocal microscope and analyzed with Leica SP2 LCS software.

Immunohistochemistry

Brains were fixed in 4% paraformaldehyde and processed for immunostaining as described previously (Qin et al. 2004). Dopaminergic neurons were detected with the polyclonal antibody against TH. Microglia were stained with rabbit anti-Iba1 antibody. NADPH oxidase membrane subunit gp91^{phox} (NOX2) was immunostained with monoclonal anti-mouse gp91^{phox} antibody. Astroglia were stained with polyclonal rabbit anti-glial fibrillary acidic protein (GFAP). Immunostaining was visualized by using 3,3′-diaminobenzidine (DAB) and urea-hydrogen peroxide tablets or nickel-enhanced DAB or Alexa Fluor 488 (green) and 555 (red) dye.

In situ visualization of O_2^- and O_2^- - derived oxidant production

In situ visualization of O_2^- and O_2^- - derived oxidant (ROS) production was assessed by hydroethidine histochemistry (Bindokas et al. 1996; Wu et al. 2003). Mice were injected with hydroethidine (10 mg/kg, i.p.) in 0.5% carboxymethyl cellulose at the time points indicated. Brains were harvested 30 min later and frozen sections (15 μm) were examined for hydroethidine oxidation product, ethidium accumulation, and fluorescence microscopy (excitation 510 nm; emission 580 nm).

Real-time RT-PCR analysis

Total RNA was extracted from the mouse midbrain samples 24 hr after LPS or saline treatment and used for reverse transcription PCR analysis as described previously (Qin et al. 2004). The primer sequences used in this study were as follows:

Table 2

Real-time PCR Primers

	Primer pairs
Mouse Iba1	5′-CTTGAAGCGAATGCTGGAGAA-3′ 5′-GGAGCCACTGGACACCTCTCT-3′
Mouse gp91^{phox} (NOX2)	5′-CAGGAGTTCCAAGATGCCTG-3′ 5′-GATTGGCCTGAGATTCATCC-3′
Mouse β-actin	5′-GTA TGA CTC CAC TCA CGG CAA A-3′ 5′-GGT CTC GCT CCT GGA AGA TG-3′

The SYBR green DNA PCR kit (Applied Biosystems, Foster City, CA) was used for real-time PCR analysis. The relative differences in expression between groups were expressed using cycle time (Ct) values normalized with β-actin, and relative differences between

control and treatment group were calculated and expressed as relative increases setting control as 100%.

TNFα, IL-1β and MCP-1 assay

Frozen brains were homogenized in 100 mg tissue/ml cold lysis buffer (20 mM Tris, 0.25M sucrose, 2 mM EDTA, 10 mM EGTA, 1% Triton X-100) and 1 tablet of Complete Mini protease inhibitor cocktail tablets/10 ml (Roche Diagnostics, Indianapolis, IN). Samples were centrifuged at 100,000 × g for 40 min. Supernatant was collected for protein assay using the BCA protein assay reagent kit (PIERCE, Milwaukee, WI). The levels of TNFα, IL-1β and MCP-1 in brains were measured with mouse TNFα, IL-1β and mouse JE/MCP-1 commercial enzyme-linked immunosorbent assay (ELISA) kits from R&D Systems (Minneapolis, MN), as described previously (Gu et al. 1998).

Statistical analysis

The data are expressed as the mean ± SEM and statistical significance was assessed with an ANOVA followed by Bonferroni's t-test. A value of $P < 0.05$ was considered statistically significant.

RESULTS

NOX2 contributes to systemic LPS-induced loss of dopaminergic neurons in the substantia nigra

To investigate the role of NOX-generated ROS in LPS-induced neurodegeneration, $NOX2^{+/+}$ and $NOX2^{-/-}$ mice were injected intraperitoneally with LPS (5 mg/kg) or saline. The brains were removed 10 months after LPS treatment, and coronal sections that encompass the entire SN were taken. The sections were immunostained with an antibody against TH to detect dopaminergic neurons in substantial nigra pars compacta (SNpc). Immunohistochemical analysis for TH immunoreactivity (+IR) indicated that systemic LPS injection caused a 39% ($p<0.01$) loss of TH+IR neurons in the SN of $NOX2^{+/+}$ mice 10 months after LPS (12 months old) compared to age matched saline controls (Fig. 1). Transgenic $NOX^{-/-}$ 12 month old control mice had similar levels of TH+IR neurons in SN to $NOX2^{+/+}$control mice, however TH+IR neurons in the SN of LPS treated $NOX2^{-/-}$ mutants were decreased 11%, which was not statistically different from either control groups. These findings suggest that NOX contributes to degeneration of dopaminergic neurons in the SN.

NOX2 mediates microglial activation in response to systemic LPS administration

Microglia initiate neuroimmune responses in brain and contribute to amplification of proinflammatory responses associated with morphologically distinct stages of activation (Block and Hong 2005; Block and Hong 2007; Crews et al. 2011). We investigated Iba1, a specific marker for microglia and other monocyte-like cells. Although Iba1 expression is increased during activation, Iba1+IR labels all microglia regardless of activation state allowing morphological assessments of activation (Ito et al. 1998). Iba1 mRNA was significantly upregulated about 2.5 fold in $NOX2^{+/+}$ mice, but not in $NOX2^{-/-}$ mice (Fig. 2A). Microglia Iba1+IR morphology, an indicator of microglia activation state, found Iba1+IR cells in 2 month old $NOX2^{+/+}$ and $NOX2^{-/-}$ mice injected with saline had small cell bodies with thin, highly ramified processes, consistent with the morphology of resting microglia. However, Iba1+IR morphology in $NOX2^{+/+}$ mice injected with LPS (5 mg/kg, i.p.) displayed the characteristics of activated amoeboid microglia, increased cell bodies, irregular shape, and intensified Iba1+IR. Human brain microglia from subjects with sepsis show similar Iba1+IR cytoplasmic hypertrophy characteristic of activated microglia (Streit

et al. 2009). In contrast, LPS activation of microglia was significantly less pronounced in the SN of $NOX2^{-/-}$ mice (Fig. 2B). In addition, LPS induction of brain TNFα mRNA was blunted (i.e. 134±13 and 80±7 fold ($p<0.01$) in $NOX2^{+/+}$ and $NOX2^{-/-}$ mice, respectively (data not shown). Interestingly, LPS induced serum TNFα was almost identical between $NOX2^{+/+}$ and $NOX2^{-/-}$ mice suggesting our high dose intraperitoneal LPS activated TNFα release from gut-blood monocytes, and/or other cells that increase blood TNFα that are not impacted by NOX2 (Supplementary Fig. 1). The reduced induction of Iba1 and TNFα mRNA and microglial activation morphology in $NOX2^{-/-}$ mice further support an important role for NOX in activation of microglia, a key initial step in neuroimmune activation and neurodegeneration.

Microglial morphology defined activation states provides an index of neuroimmune activation in models of neurodegeneration. We investigated the long term impact of LPS treatment at multiple points up to 10 months after LPS treatment in $NOX2^{+/+}$ mice (Fig. 3). LPS treatment of 2 month old $NOX2^{+/+}$ mice resulted in a rapid increase in activated morphology Iba1+IR cells within 1 hr that persisted at 24 hr. In the saline control groups, microglia at 1, 3, and 24 hr have a resting morphology, small cell bodies with thin, highly ramified processes. However, saline controls showed age-related increases in microglial activation at 4, 9 and 12 months of age (Fig. 3). LPS treated mice showed greater numbers of activated microglia for up to 10 months after LPS treatment, i.e. 4 to 12 months of age (2–10 months after LPS) that paralleled saline control age-related increases in activated microglial morphology. Interestingly, control mice at 12 months of age had similar levels of activated microglia as LPS treated animals at 4 months of age (i.e. 2 months after LPS treatment) (Fig. 3). These results indicate activation of brain microglia by LPS persists for long periods that further increase in parallel with age related increases in microglial activation.

Increased NOX expression and ROS production

We have previously found that NOX induction is associated with markers of neuronal death in both mouse and human brain (Qin and Crews 2012b). NOX2 is a membrane subunit ($gp91^{phox}$) of NADPH oxidase (NOX), the enzyme complex responsible for the respiratory burst of reactive oxygen species (ROS) that occurs in activated phagocytes. Activation of this enzyme in microglia induces the production of ROS, resulting in dopaminergic neurotoxicity in mixed glial-neuronal cultures (Qin et al. 2004). We determined NOX2 ($gp91^{phox}$) mRNA and NOX2+IR cells in brain. Treatment of C57BL/6 mice with LPS resulted in a 12 fold increase in NOX2 mRNA in midbrain at 24hr (Fig. 4A). NOX2+IR cells are small and rare in controls. In LPS treated mice NOX2+IR cells were increased about 5.5 fold in SN at 24hr (Fig. 4B), consistent with rapid induction of NOX2 mRNA and protein. NOX2+IR cells include large and small phenotypes that likely include microglia and other brain cell types. Interestingly, NOX2+IR cells increased at 10 and 20 months in saline controls with some showing neuron-like morphology (4B, 4C). In LPS treated mice, NOX2+IR cells also increased with age in parallel with saline controls. NOX2+IR cells were 5.8 and 6.5 fold greater than age matched controls at 10 and 20 months, respectively. NOX2+IR cells in SN 10 and 20 months after LPS show distinct neuron-like large triangular morphology with processes (Fig. 4C). These findings indicate NOX induction increases rapidly in brain following LPS treatment, and continues to increase with age through an induction in neuron-like large cells as well as smaller glial cells.

NOX2 is the catalytic subunit of NADPH oxidase that produces superoxide that is linked to ROS and oxidative stress. To investigate oxidative stress within mouse brain, we used a histochemical method that allows in situ visualization of O_2^- and O_2^--derived oxidant production by dihydroethidium (DHE), a lipophilic ROS-sensitive dye that crosses the blood brain barrier allowing localization of superoxide and other ROS in brain (Murakami et al.

1998; Zielonka et al. 2009), although changes in the blood brain barrier might impact responses. DHE is converted to fluorescent ethidium at the sites of formation of superoxide and ROS. In 2 month old saline control mice, production of O_2^- and O_2^--derived oxidants, evidenced by ethidium fluorescence, was very low at 1h and 24hr. Aging saline control mice showed increased age-related ethidium fluorescence (ROS) at 12 and 22 months of age (10 and 20 months after saline) (Fig. 5), compared with 2 month-old mice. LPS treatment rapidly increased ROS production many fold at 1 and 24hr. At 1 hr both small and large cells show red fluorescence with both cell phenotypes increasing by 24 hr. Both saline and LPS treated mice show distinct red cellular phenotypes at 12 and 22 months of age (10 and 20 months after LPS). LPS treated animals 10 and 20 months after treatment show large highly labeled sites larger than any single cell. Although LPS induced ROS fluorescent intensity 24 hr after LPS only slightly increased over the next 10 months, ROS fluorescence almost doubled as LPS treated mice aged from 12–22 months (i.e. 10–20 months after LPS) (Fig. 5). These results indicate LPS causes persistent increases in ROS in SN that further increase with age.

NOX and ROS cellular localization

To further investigate induction of NOX and production of ROS, we performed triple immunohistochemistry using antibodies to $gp91^{phox}$ (NOX2) and Iba1, a microglial marker, TH, a marker of dopaminergic neurons or GFAP, a marker of astrocytes on brain sections from the mice injected with dihydroethidium 10 months after systemic LPS treatment. As shown in figure 6A, TH+IR cells (green) show fragmented dysmorphology consistent with degeneration. NOX $gp91^{phox}$+IR cells (blue)and ROS (red) are triple-labeled with TH+IR cells (green) that in the merged panel identifies overlapping blue-red-green cells as white. We found that both TH, the dopaminergic neuron marker, and Iba1, the microglial marker showed prominent overlap with NOX2 and ROS, but not with the astrocyte marker GFAP +IR (green) as shown in Figure 6A and 6B. These results indicate that NOX expression and ROS production predominantly occurred in microglia and dopaminergic neurons in the substantia nigra 10 months after LPS treatment.

DPI suppresses microglial activation, ROS generation and production of proinflammatory cytokines

To further investigate the role of NOX in neuroimmune activation, we studied diphenyleneiodonium (DPI, 3 mg/kg, i.p.), a non-specific inhibitor of oxidases known to block NOX, in 4 month old mice, 2 months after LPS treatment. Iba1+IR microglial activated morphology were found in the LPS-treated group, however, in the LPS and DPI co-treated group, Iba1+IR cells displayed resting morphology, similar to saline and DPI alone (Fig. 7). Assessment of ethidium fluorescence (ROS) indicated as expected that DPI treatment reduced ROS formation in LPS treated mice (Fig. 8A). Further, LPS treatment caused long-lasting elevated levels of TNFα, IL-1β and MCP-1protein in mouse brain as determined by ELISA. Among these proinflammatory cytokines, IL-1β remained increased many fold 2 months after LPS treatment. DPI treatment significantly reduced TNFα, IL-1β and MCP-1 protein in LPS treated mice (Fig. 8B). These data suggest that NOX activation and persistent ROS are essential for persistent microglial activation and elevation of proinflammatory cytokines.

DISCUSSION

We report here that the slow progressive LPS-induced loss of SN dopaminergic neurons in vivo is blunted in $NOX2^{-/-}$ mice 10 months after LPS treatment. Further, LPS induced microglial activation was reduced in $NOX2^{-/-}$ mice. We have previously found that LPS induced brain TNFα persisted for at least 10 months in association with SN

neurodegeneration (Qin et al. 2007). More extensive studies indicated a slow progressive SN TH neuron loss, that after 7 months was significantly reduced by about 25% (Liu et al. 2008; Qin et al. 2007). In female mice, resistant to SN TH loss, monthly LPS increased SN degeneration and caused L-DOPA reversible motor dysfunction (Liu et al. 2008). In mice microglial and NOX2 activation coincide with neuronal death that is blocked by NOX inhibitors (Qin and Crews 2012b). We report here that DPI inhibition of ROS formation is able to reverse microglial activation and elevated levels of proinflammatory cytokines following two months of persistent activation. These results support the hypothesis that activation of NOX and formation of ROS drive persistent brain microglial neuroimmune activation, NOX2 induction and ROS formation that contribute to SN dopaminergic neurodegeneration.

We studied microglial morphology at multiple ages from young adults (e.g. 2 months of age) to elderly adults (e.g. 22 months of age) and found age related increases in microglial activation, NOX2 expression and ROS production in both healthy controls and LPS treated mice. LPS treated mice showed rapid increases in microglial activation morphology, NOX2 expression, and ROS formation within hours that persisted for days and months. Controls at 4 months of age began to show slight increases in microglial activation morphology that increased with age such that 10 month saline control brain activated microglia were similar to LPS treated mice at 4 months old. LPS treated animals also showed age related increases in activation remaining persistently elevated, compared to age matched controls. Senescent microglial activation morphology is confounded by dystrophic (Streit et al. 2009) and/or acquired deactivation states (Colton 2009) that could contribute to our findings of age related increases in microglial activation morphology. Regardless, our findings indicate that LPS induced microglial activation persists for almost the entire lifespan of mice and could underlie the increased incidence of neurodegenerative diseases with increasing age, particularly PD.

Expression of NOX2 and production of ROS also increased with age at 12 and 22 months (10 and 20 months after LPS). However, LPS treated mouse brains showed increasingly greater increases in NOX2 and ROS with age compared to controls consistent with acceleration and amplification of NOX2 oxidative stress with age. This differs from the parallel increases in microglial activation with age from 4 to 22 months between control and LPS groups. Interestingly, we found expression of NOX2 in 12 and 22 month old animals appeared to increase primarily in large cells having neuron-like morphologies. Further, ROS determinations found increasingly large ROS marked complexes in older animals of both groups. Confocal microscopy using cell type specific markers found that TH+IR cells colocalized with ROS and NOX2 (gp91) in brains of LPS treated mice 10 months after treatment indicating oxidative stress is increasing within SN TH neurons (Fig. 6). Microglia also showed co-localization with NOX2 and ROS. These findings are consistent with our hypothesis that persistent neuroimmune activation involves ROS formed from NOX2 that with increasing age results in amplified oxidative stress and SN TH neuron degeneration (Fig. 9).

In summary, LPS increases SN NOX2 expression, ROS production and microglial activation that persist for long periods and perhaps the lifetime. Age also leads to increases in neuroimmune activation. LPS and age act synergistically in old mice, increasing NOX2 expression and ROS formation that likely contribute to increased SN neurodegeneration during aging.

Supplementary Material

Refer to Web version on PubMed Central for supplementary material.

Acknowledgments

This work was supported by grants from National Institute of Health, National Institute of Environmental Health Sciences and the National Institute on Alcohol Abuse and Alcoholism [AA020023, AA020024, AA020022, AA019767, AA11605 and AA007573] and the Bowles Center for Alcohol Studies. This work was also supported in part by the Intramural Research Program of the NIH/NIEHS. The authors thank Michelle L. Block and Belinda Wilson for their technical support and thank Diana Lotito for assisting with the manuscript preparation.

References

Bindokas VP, Jordan J, Lee CC, Miller RJ. Superoxide production in rat hippocampal neurons: selective imaging with hydroethidine. J Neurosci. 1996; 16:1324–36. [PubMed: 8778284]

Block ML, Hong JS. Microglia and inflammation-mediated neurodegeneration: multiple triggers with a common mechanism. Prog Neurobiol. 2005; 76:77–98. [PubMed: 16081203]

Block ML, Hong JS. Chronic microglial activation and progressive dopaminergic neurotoxicity. Biochem Soc Trans. 2007; 35:1127–32. [PubMed: 17956294]

Chen WJ, Parnell SE, West JR. Neonatal alcohol and nicotine exposure limits brain growth and depletes cerebellar Purkinje cells. Alcohol. 1998; 15:33–41. [PubMed: 9426835]

Colton CA. Heterogeneity of microglial activation in the innate immune response in the brain. Journal of neuroimmune pharmacology: the official journal of the Society on NeuroImmune Pharmacology. 2009; 4:399–418. [PubMed: 19655259]

Crews FT, Nixon K, Wilkie ME. Exercise reverses ethanol inhibition of neural stem cell proliferation. Alcohol. 2004; 33:63–71. [PubMed: 15353174]

Crews FT, Zou J, Qin L. Induction of innate immune genes in brain create the neurobiology of addiction. Brain Behav Immun. 2011; 25(Suppl 1):S4–S12. [PubMed: 21402143]

Dauer W, Przedborski S. Parkinson's disease: mechanisms and models. Neuron. 2003; 39:889–909. [PubMed: 12971891]

Gao HM, Liu B, Zhang W, Hong JS. Critical role of microglial NADPH oxidase-derived free radicals in the in vitro MPTP model of Parkinson's disease. Faseb J. 2003; 17:1954–6. [PubMed: 12897068]

Glass CK, Saijo K, Winner B, Marchetto MC, Gage FH. Mechanisms underlying inflammation in neurodegeneration. Cell. 2010; 140:918–34. [PubMed: 20303880]

Gu L, Okada Y, Clinton SK, Gerard C, Sukhova GK, Libby P, Rollins BJ. Absence of monocyte chemoattractant protein-1 reduces atherosclerosis in low density lipoprotein receptor-deficient mice. Mol Cell. 1998; 2:275–81. [PubMed: 9734366]

Hirsch EC, Hunot S. Neuroinflammation in Parkinson's disease: a target for neuroprotection? Lancet Neurol. 2009; 8:382–97. [PubMed: 19296921]

Ito D, Imai Y, Ohsawa K, Nakajima K, Fukuuchi Y, Kohsaka S. Microglia-specific localisation of a novel calcium binding protein, Iba1. Brain Res Mol Brain Res. 1998; 57:1–9. [PubMed: 9630473]

Li G, Liu Y, Tzeng NS, Cui G, Block ML, Wilson B, Qin L, Wang T, Liu B, Liu J, et al. Protective effect of dextromethorphan against endotoxic shock in mice. Biochem Pharmacol. 2005; 69:233–40. [PubMed: 15627475]

Liu Y, Qin L, Wilson B, Wu X, Qian L, Granholm AC, Crews FT, Hong JS. Endotoxin induces a delayed loss of TH-IR neurons in substantia nigra and motor behavioral deficits. Neurotoxicology. 2008; 29:864–70. [PubMed: 18471886]

McClain JA, Morris SA, Deeny MA, Marshall SA, Hayes DM, Kiser ZM, Nixon K. Adolescent binge alcohol exposure induces long-lasting partial activation of microglia. Brain, behavior, and immunity. 2011; 25(Suppl 1):S120–8.

McGeer PL, Yasojima K, McGeer EG. Inflammation in Parkinson's disease. Adv Neurol. 2001; 86:83–9. [PubMed: 11554012]

Murakami K, Kondo T, Kawase M, Li Y, Sato S, Chen SF, Chan PH. Mitochondrial susceptibility to oxidative stress exacerbates cerebral infarction that follows permanent focal cerebral ischemia in mutant mice with manganese superoxide dismutase deficiency. J Neurosci. 1998; 18:205–13. [PubMed: 9412501]

Paxinos, G.; Franklin, KB. The Mouse Brain in Sterotaxic Coordinates. Elsevier Academic Press; 2004.

Qian L, Flood PM, Hong JS. Neuroinflammation is a key player in Parkinson's disease and a prime target for therapy. Journal of neural transmission. 2010; 117:971–9. [PubMed: 20571837]

Qin L, Crews FT. Chronic ethanol increases systemic TLR3 agonist-induced neuroinflammation and neurodegeneration. Journal of neuroinflammation. 2012a; 9:130. [PubMed: 22709825]

Qin L, Crews FT. NADPH oxidase and reactive oxygen species contribute to alcohol-induced microglial activation and neurodegeneration. Journal of neuroinflammation. 2012b; 9:5. [PubMed: 22240163]

Qin L, He J, Hanes RN, Pluzarev O, Hong JS, Crews FT. Increased systemic and brain cytokine production and neuroinflammation by endotoxin following ethanol treatment. J Neuroinflammation. 2008; 5:10. [PubMed: 18348728]

Qin L, Liu Y, Wang T, Wei SJ, Block ML, Wilson B, Liu B, Hong JS. NADPH oxidase mediates lipopolysaccharide-induced neurotoxicity and proinflammatory gene expression in activated microglia. J Biol Chem. 2004; 279:1415–21. [PubMed: 14578353]

Qin L, Wu X, Block ML, Liu Y, Breese GR, Hong JS, Knapp DJ, Crews FT. Systemic LPS causes chronic neuroinflammation and progressive neurodegeneration. Glia. 2007; 55:453–62. [PubMed: 17203472]

Streit WJ, Braak H, Xue QS, Bechmann I. Dystrophic (senescent) rather than activated microglial cells are associated with tau pathology and likely precede neurodegeneration in Alzheimer's disease. Acta Neuropathol. 2009; 118:475–85. [PubMed: 19513731]

Wu DC, Teismann P, Tieu K, Vila M, Jackson-Lewis V, Ischiropoulos H, Przedborski S. NADPH oxidase mediates oxidative stress in the 1-methyl-4-phenyl-1,2,3,6-tetrahydropyridine model of Parkinson's disease. Proc Natl Acad Sci U S A. 2003; 100:6145–50. [PubMed: 12721370]

Zhang W, Wang T, Qin L, Gao HM, Wilson B, Ali SF, Hong JS, Liu B. Neuroprotective effect of dextromethorphan in the MPTP Parkinson's disease model: role of NADPH oxidase. FASEB journal: official publication of the Federation of American Societies for Experimental Biology. 2004; 18:589–91. [PubMed: 14734632]

Zielonka J, Hardy M, Kalyanaraman B. HPLC study of oxidation products of hydroethidine in chemical and biological systems: ramifications in superoxide measurements. Free radical biology & medicine. 2009; 46:329–38. [PubMed: 19026738]

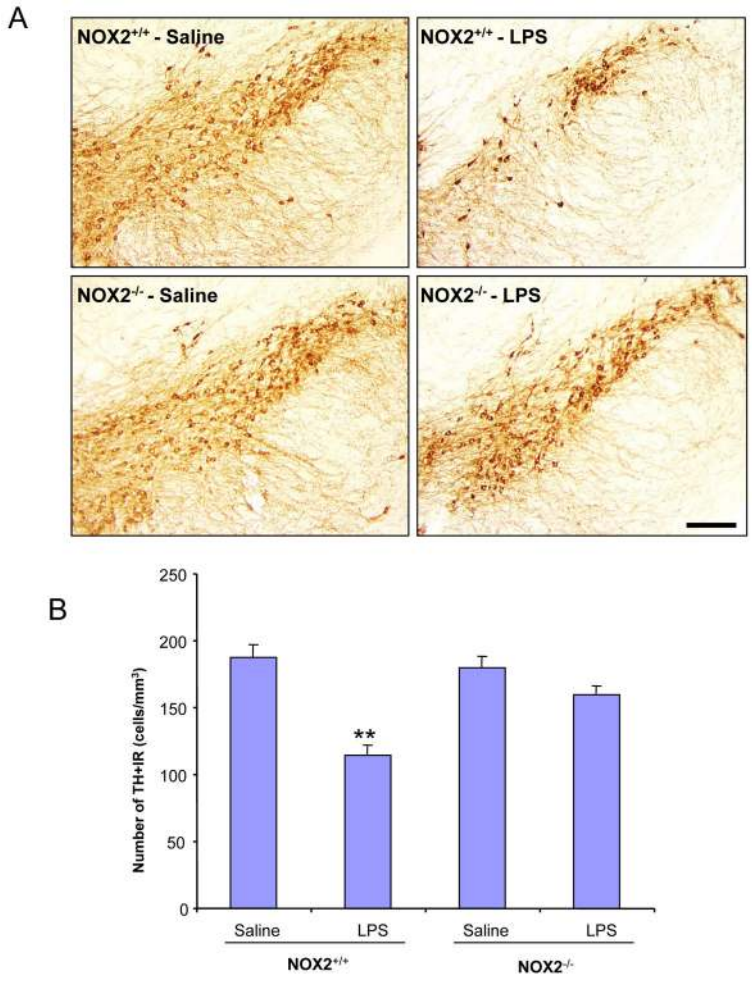

Fig. 1.

NOX2-deficient mice are more resistant to systemic LPS-induced neurotoxicity. Eight-week-old male C57BL/6 ($NOX2^{+/+}$) and Cybb ($NOX2^{-/-}$) mice were intraperitoneally injected with a single dose of LPS (5 mg/kg, i.p.) or saline and then maintained under normal conditions. Mice were sacrificed and brain sections (35 μm) that encompass the entire substantia nigra (SN) were collected 10 months after LPS or saline injection. After immunostaining with TH antibody, the number of TH+IR neurons in the substantia nigra pars compacta (SNpc) was counted as described in methods. (A) Visualization of TH+IR neurons in the substantia nigra (SN) of saline and LPS-treated animals. Scale bar=200 μM. (B) Number of TH+IR neurons in the SN of saline and LPS-treated $NOX2^{+/+}$ and $NOX2^{-/-}$ mice. Systemic LPS injection caused a greater loss of TH+IR neurons in the SN of $NOX2^{+/+}$ mice than that of $NOX2^{-/-}$ mice, compared with the corresponding saline controls. ** $P < 0.01$, compared with the corresponding saline controls.

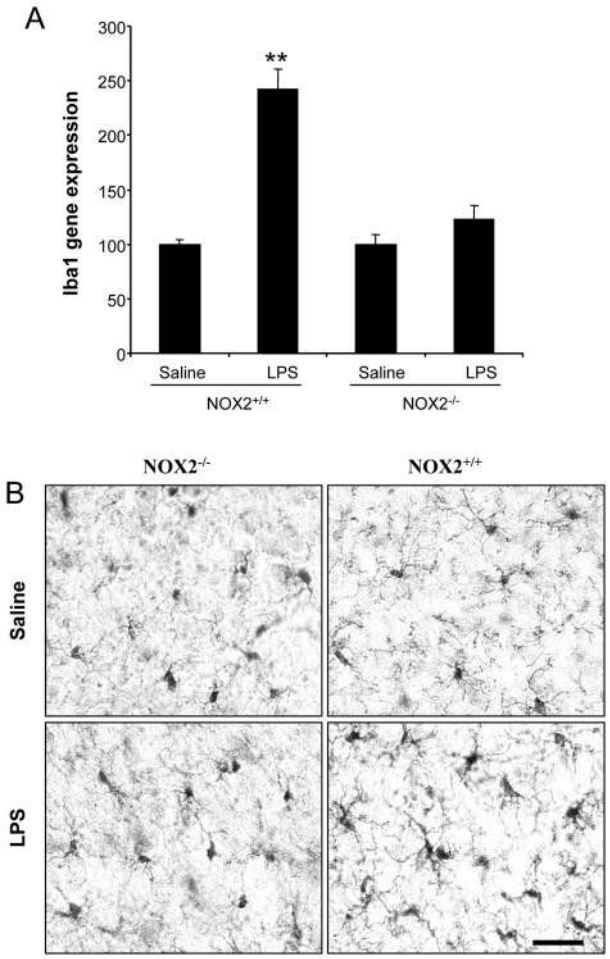

Fig. 2.

Immunocytochemical analysis of microglia. NOX2$^{+/+}$ and NOX2$^{-/-}$ mice were sacrificed 1 hr following saline or LPS (5 mg/kg, i.p.). (A) Iba1 mRNA in midbrain was determined by real-time PCR. Systemic LPS treatment significantly upregulated Iba1 gene expression in NOX2$^{+/+}$ mice, but not in NOX2$^{-/-}$ mice. (B) Brain sections were immunostained with an antibody against Iba1, a specific microglial marker. Activated microglia in substantia nigra were shown by increased cell size, irregular shape and intensified Iba1 staining in LPS-treated NOX2$^{+/+}$ mouse brains. The images presented are representative of three independent experiments. Scale bar=50μM.

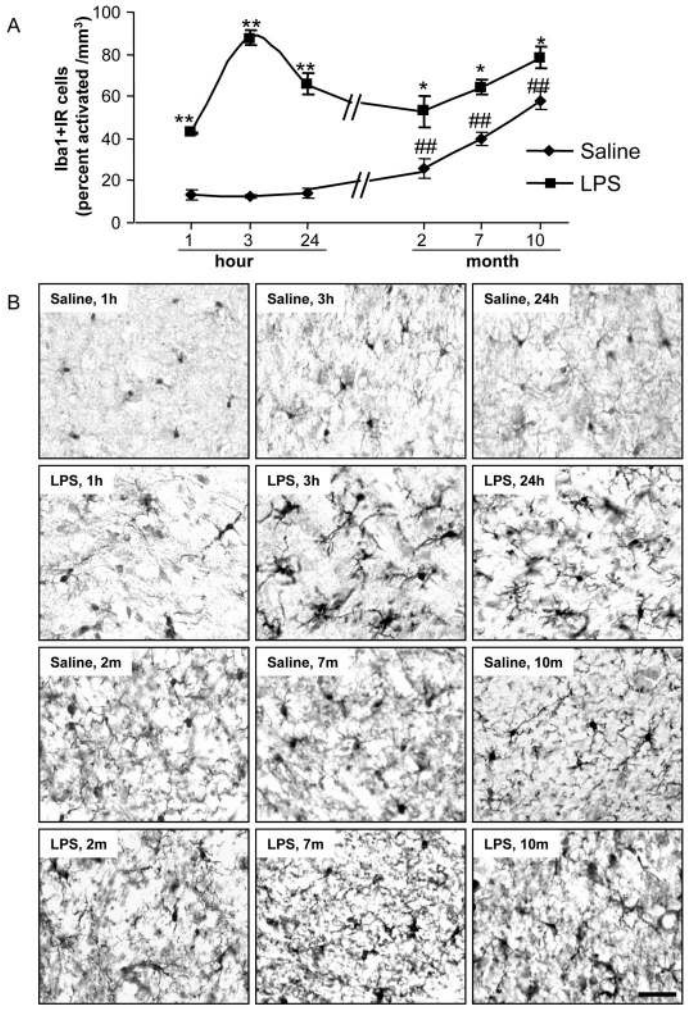

Fig. 3.

Time course of microglial response to systemic LPS treatment. Male C57BL/6 mice were injected with saline or LPS (5 mg/kg, i.p.) and sacrificed at the time points indicated. Brain sections were immunostained with Iba1 microglial antibody. (A) Quantification of activated Iba1+IR cells in substantia nigra. LPS groups at all the time points studied increased the fraction of activated microglia with a peak at 3 hr. Age-related percent activated Iba1+IR cells were significantly increased at 2, 7 and 10 months after saline injection (4, 9 and 12 months of age). (B) Representative images from saline and LPS-treated mice. LPS groups showed persistent activation of microglia with the largest morphological changes at 3 hr. In the saline control groups, microglia at 1, 3, and 24 hr have a resting morphology: small cell bodies with thin, highly ramified processes. However, at 2, 7 and 10 months some microglia were activated, large cell bodies, irregular shape and intensified Iba1 staining. *P<0.05, **P<0.01, compared with the corresponding saline control group. ##P<0.01, compared with 1h saline group. Scale bar=50μm.

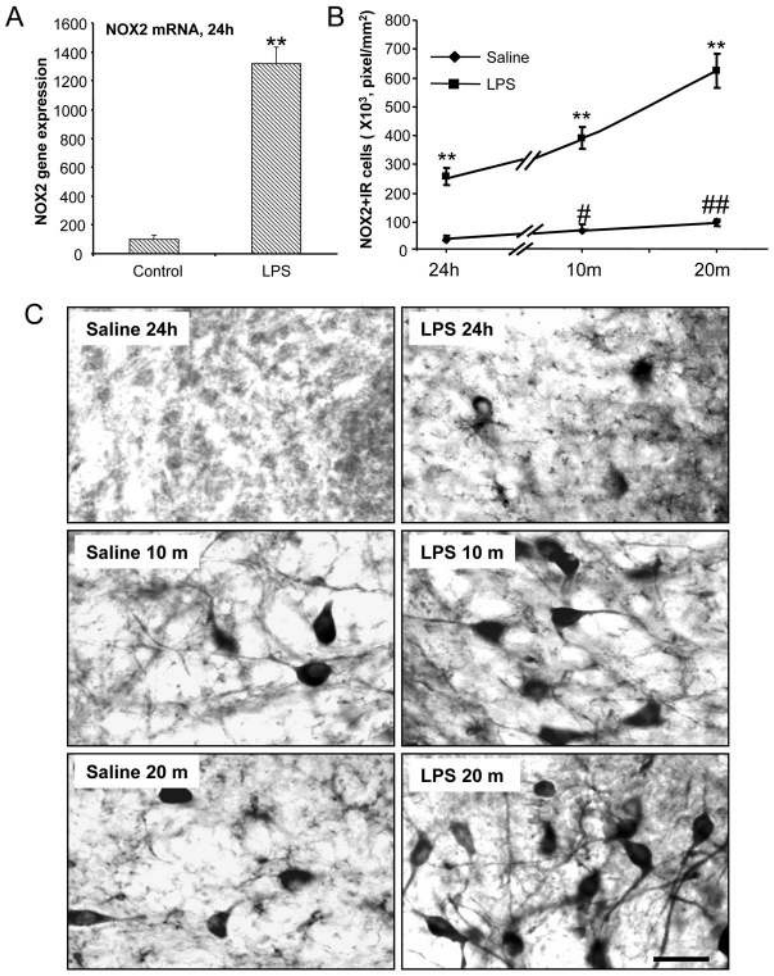

Fig. 4.

Systemic LPS increases brain NOX2 expression. Male C57BL/6 mice were injected with LPS (5 mg/kg, i.p.) or saline and sacrificed at 24 hr, 10 and 20 months following LPS treatment. (A) NOX2 gene expression in the midbrain was determined by real-time PCR. NOX2 mRNA was significantly increased 24 hr after LPS treatment. (B) Brain sections were immunostained with monoclonal mouse NOX2 antibody, which did not stain NOX2$^{-/-}$ mouse brain. The level of NOX2 immunoreactivity in SN was quantified by BioQuant image analysis system. Systemic LPS significantly enhanced NOX2 immunoreactivity at 24 hr, 10 and 20 months. (C) The images shown are representative ofNOX2+IR cells from control and LPS groups. Age-related NOX2 up-regulation was observed at 10 and 20 months in saline control mice. Scale bar=30μm. **P < 0.01, compared with the corresponding saline control mice, $^{\#}$P<0.05, $^{\#\#}$P<0.01, compared with 24 hr saline control mice.

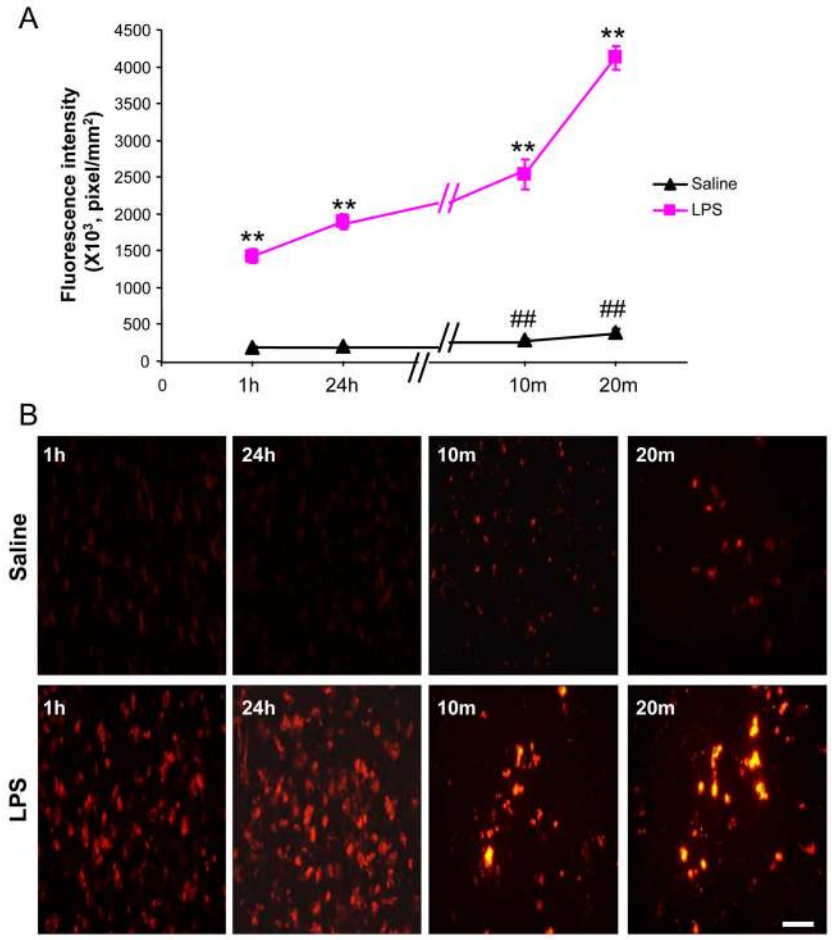

Fig. 5.

Systemic LPS treatment induces ROS production at 1 and 24 hr and remains elevated at 10 and 20 months. Mice were injected with hydroethidine (10 mg/kg, i.p.) 0.5hr, 23.5 hr, 10 months and 20 months after a single i.p. injection of LPS. Brains were harvested 30 min later and frozen sections (15μm) were examined for hydroethidine oxidation product, ethidium accumulation, by fluorescence microscopy. (A) Level of fluorescence intensity of ethidium was quantified by BioQuant image analysis software. (B) Images of ethidium fluorescence. Systemic LPS treatment significantly induced O_2^- and O_2^--derived oxidant production (ROS) 1 and 24hr and remains elevated 10 and 20 months after LPS injection, compared with the corresponding saline controls. Age-related ROS production was enhanced at 10 and 20 months in saline control mice, ** $P < 0.01$, compared with the corresponding saline control group. ## $P < 0.01$, compared with 1 hr saline group. Scale bar=200 μM.

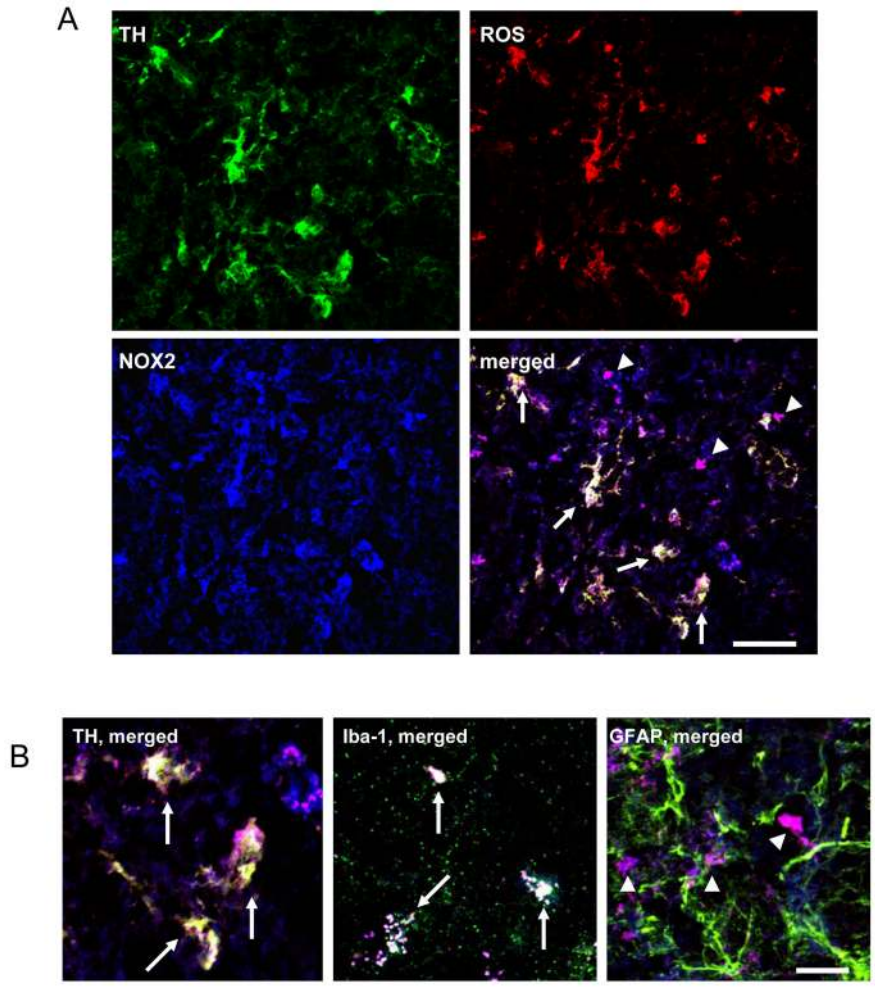

Fig. 6.

Colocalization of NOX2 expression and ROS production. Mice were injected with hydroethidine (10 mg/kg, i.p.) 10 months after a single dose of LPS i.p. injection. Brains were harvested 30 min later and frozen sections (15 μm) were double-labeled for NOX2 (blue) and Iba1 (green), NOX2 (blue) and TH (green) as well as NOX2 (blue) and GFAP (green) to analyze triple labeling or colabeling by using the Leica SP2 LCS confocal software. Confocal microscopy shows that NOX2+IR cells and ROS are triple-labeled with TH (A-merged, the right lower panel and B-merged, the left panel) or Iba1 (B-merged, the middle panel) in white with arrows, indicating NADPH oxidase (NOX) subunit NOX2 ($gp91^{phox}$) activation and ROS production predominantly occurred in DA neurons and microglial cells. Conversely, NOX2+IR cells and ROS are little glial fibrillary acidic protein (GFAP) positive. Double-labeled representative images are shown in pink with arrow heads indicating the colabeling of NOX2 with ROS (A-merged, the right lower panel; B-merged, the right panel). In Fig. 6A, Scale bar=30μm. In Fig. 6B, Scale bar=20μm.

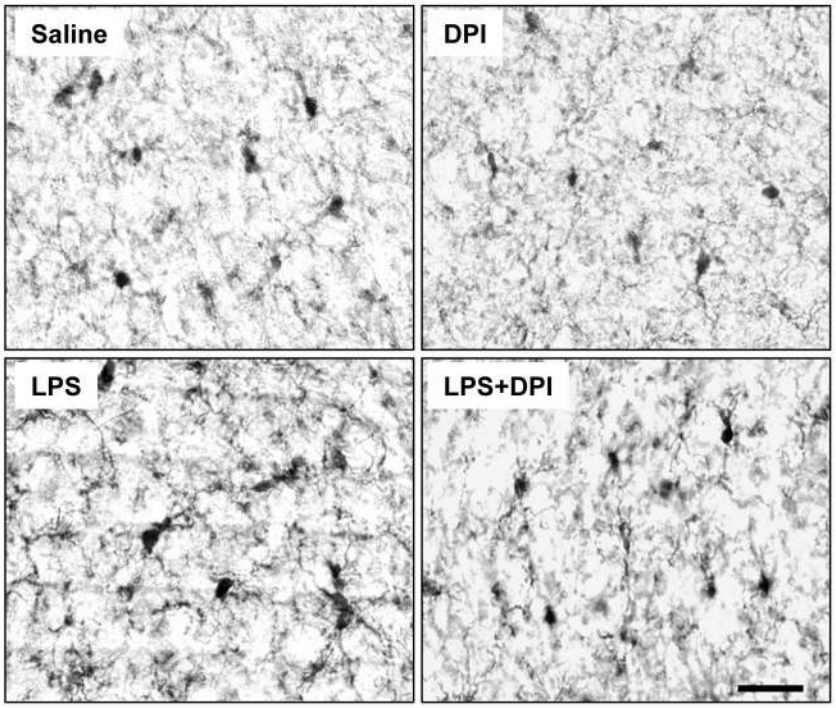

Fig. 7.

Diphenyleneiodonium (DPI) blocks LPS-induced microglial activation. Male C57BL/6 mice were treated with LPS (5 mg/kg, i.p.) or saline. DPI (3 mg/kg) was injected intraperitoneally on two consecutive days 2 months after LPS treatment. Mice were sacrificed 3 hr after the last dose of DPI. Brain sections were stained with Iba1 antibody. Systemic LPS markedly caused microglial activation. In the saline or DPI treated mice, most of the microglia were in a resting morphological shape. Iba1+IR cells in LPS-treated mouse brains were activated as shown by increased cell size, irregular shape, and intensified Iba1 staining. DPI blocked LPS-induced microglial activation shown by a resting morphological shape. Scale bar=50μm.

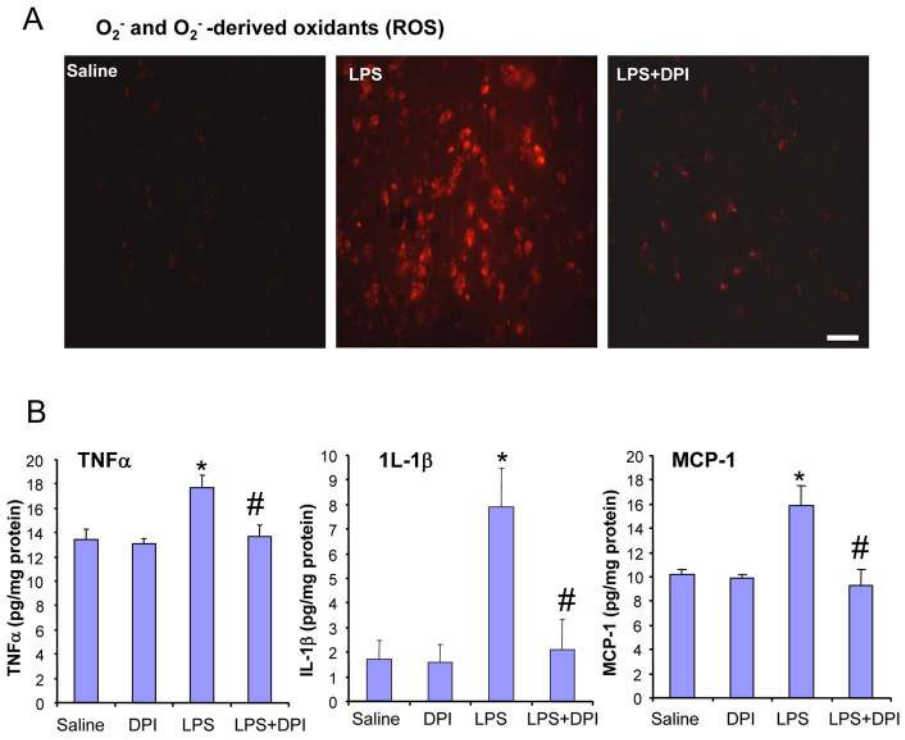

Fig. 8.

Diphenyleneiodonium (DPI) inhibits LPS-induced production of ROS, TNFα, IL-1β, and MCP-1. Male C57BL/6 mice were treated with LPS (5 mg/kg, i.p.) or saline. DPI (3 mg/kg) was applied intraperitoneally on two consecutive days 2 months after LPS treatment. Mice were sacrificed 3 hr after the last dose of DPI. Brain O_2^- and O_2^--derived oxidants (ROS), TNFα, IL-1β, and MCP-1 were measured as described in materials and methods. (A) Representative images of O_2^- and O_2^--derived oxidants in SN. DPI significantly reduced LPS-induced production of O_2^- and O_2^--derived oxidants. Scale bar=30μm. (B) Systemic LPS treatment significantly increased production of TNFα, IL-1β, and MCP-1 compared with saline controls. DPI significantly reduced LPS-induced increases in production of TNFα, IL-1β, and MCP-1. * $P < 0.05$, compared with the saline control mice, $^{\#}P < 0.05$, compared with the LPS-treated mice.

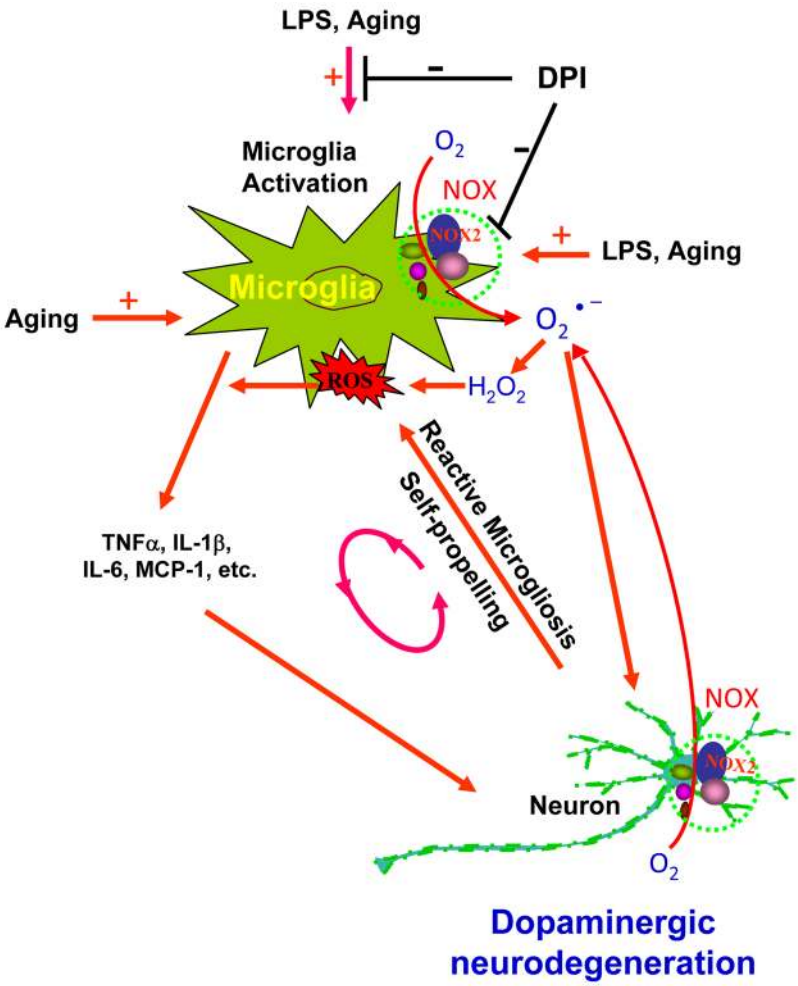

Fig. 9.

NOX-ROS is a key signaling in systemic LPS-induced dopaminergic neurodegeneration. LPS as a pro-inflammatory trigger activates microglia to release neurotoxic factors, such as TNFα, IL-1β, MCP-1, and ROS (O_2^-). Among these pro-inflammatory factors, ROS have been implicated as key mechanisms of LPS neurotoxicity. Further, damaged or dying neurons have the potential to prime microglia to become more sensitive to additional stimuli and result in an exaggerated and prolonged proinflammatory response that enhances neuronal damage (i.e. reactive microgliosis). NOX2-deficient ($NOX2^{-/-}$) mice showed reduced DA neurotoxicity and decreased microglial activation. Blockade of NOX with DPI inhibits activation of microglia and production of ROS, TNFα, IL-1β and MCP-1. These results suggest that NOX and aging contribute to systemic LPS-elicited microglial activation, oxidative stress and dopaminergic neurodegeneration.

Table 1

Summary of antibodies used in the present study

Antibody	Manufacturer	Host	Species detected	Dilution	Application
TH	Chemicon International	Rabbit	Mouse	1:500	IHC
Iba1	Wako Pure Chemical Industries, Ltd	Rabbit	Mouse	1:1000	IHC
$gp91^{phox}$ (NOX2)	Transduction Laboratories	Mouse	Mouse	1:300	IHC
GFAP	DakoCytomation	Rabbit	Mouse	1:500	IHC

IHC, immunohistochemistry